

Electrocatalytic Activity of Co-based Perovskite Oxides for Oxygen Reduction and Evolution Reactions

Boyoon Shin, Sangwon Choi, Yongsug Tak*

Department of Chemical Engineering, Inha University, 253 Yonghyun-dong, Nam-ku, Incheon 402-751, Republic of Korea

*E-mail: ystak@inha.ac.kr

Received: 24 February 2016 / Accepted: 14 April 2016 / Published: 4 June 2016

Cathode of aqueous Li-air battery requires high electrocatalytic activities for oxygen reduction reaction and oxygen evolution reaction. Pure Co-based perovskite oxide (LaCoO_3) was prepared by an auto-combustion method at a relatively low calcination temperature (640°C), and La of $\text{La}_{1-x}\text{Sr}_x\text{CoO}_3$ was partially substituted with Sr to enhance its electrocatalytic activities. $\text{La}_{0.7}\text{Sr}_{0.3}\text{CoO}_3$ showed excellent catalytic activity for the oxygen evolution reaction, and its activity for the oxygen reduction reaction was increased with 5 wt% Pt loading. The electrochemical activity of perovskite was investigated by linear sweep voltammetry and electrochemical impedance spectroscopy.

Keywords: perovskite oxides, oxygen reduction reaction, oxygen evolution reaction, LaCoO_3 , electrochemical analysis

1. INTRODUCTION

A rechargeable Li-air battery was introduced by Abraham et al. in 1996 [1]. This type of battery has received significant attention as a next-generation battery for electric vehicles because of its theoretically high energy density, which is 10 times higher than that of Li-ion batteries [2–4]. Li-air battery can be classified as non-aqueous and aqueous based on the electrolyte used. In non-aqueous electrolyte Li-air batteries, solid Li oxides form on the air electrodes during discharging, which can prevent the inflow of O_2 . Furthermore, during discharging, the presence of undissociated Li oxides limits the cell cyclability. In contrast, in aqueous Li-air batteries, a soluble discharge product is formed, which is advantageous for extending their cyclability [5–6].

The air electrodes used in aqueous Li-air batteries should have electrocatalytic activities for the oxygen reduction reaction (ORR) $\text{O}_2 + 2\text{H}_2\text{O} + 4\text{e}^- \rightarrow 4\text{OH}^-$ —during discharging and the oxygen

evolution reaction (OER) $4\text{OH}^- \rightarrow \text{O}_2 + 2\text{H}_2\text{O} + 4\text{e}^-$ —during charging [7]. Pt is an excellent catalyst for the ORR, and Ir oxide is known to be the best material for the OER. However, electrode materials with high activities for both the ORR and OER must be identified. Transition metal oxides and perovskite oxides, ABO_3 , have been investigated as cathode materials for Li-air batteries and as alternatives to expensive noble metal catalysts, such as Pt and IrO_2 [8–9]. Perovskite oxides are promising non-noble metal and bifunctional catalysts for fuel cells and metal-air batteries because of their high catalytic activities and abundance. Perovskite oxides with various compositions can be synthesized by partially replacing the A-site and B-site cations with other metal ions. A-site substitution has been shown to influence O_2 adsorption, whereas B-site substitution affects the activity of the adsorbed O_2 [10–11]. Substituted perovskite oxides are commonly represented by the formula $\text{A}_{1-x}\text{A}'_x\text{B}_{1-y}\text{B}'_y\text{O}_3$, where A or A' is a rare-earth or alkaline-earth metal, and B or B' is a transition metal [12]. Perovskites with Co substitution in the B site show good catalytic activities because of the high oxidation state of the Co ions [13], whereas perovskites with Sr substitution in the A site exhibit good conductivity, high O_2 diffusivity, and high O_2 -dissociation ability [14–15].

In this work, perovskite oxides with various compositions were synthesized, and their activities for both the ORR and OER, which are required for air electrodes in aqueous Li-air batteries, were tested. La Co oxide (LaCoO_3) catalysts were prepared via three different methods and used for the OER. La was partially substituted with Sr ($\text{La}_{1-x}\text{Sr}_x\text{CoO}_3$) to enhance the electrocatalytic activities of LaCoO_3 . To improve the ORR activity of $\text{La}_{1-x}\text{Sr}_x\text{CoO}_3$, a hybrid-type catalyst consisting of Pt on $\text{La}_{1-x}\text{Sr}_x\text{CoO}_3$ was prepared and tested.

2. EXPERIMENTAL

2.1. Synthesis of perovskite oxide catalysts

Perovskite catalysts were prepared via three different methods: high-temperature calcination (HT), the citric acid method (CA), and the auto-combustion method (AC). The syntheses of LaCoO_3 using HT and CA were similar to the methods reported in Refs. [16–18]. To prepare LaCoO_3 via AC, La(III) nitrate hexa-hydrate ($\text{La}(\text{NO}_3)_3 \cdot 6\text{H}_2\text{O}$) and Co(II) nitrate hexa-hydrate ($\text{Co}(\text{NO}_3)_2 \cdot 6\text{H}_2\text{O}$) were dissolved in 50 mL of deionized water. Then, glycine was added to the mixture as a complexing agent, and the mixture was dried in an oven. The resulting rigid gel solution was heated to 300°C , and the auto-ignition of glycine was achieved in a vacuum oven. Finally, the obtained solid products were calcined at 640°C for 4 h under an air atmosphere [19]. $\text{La}_{1-x}\text{Sr}_x\text{CoO}_3$ ($x=0.1, 0.3, 0.5, 0.7, \text{ and } 0.9$) was synthesized via AC. The extent (x) of the Sr substitution of La was controlled by maintaining a 1.0 stoichiometric ratio of (La+Sr) to Co. A hybrid-type electrode consisting of Pt nanoparticles on $\text{La}_{1-x}\text{Sr}_x\text{CoO}_3$ was prepared by a polyol method [20].

2.2. Electrochemical analysis of perovskite oxide catalysts

The crystallinity of the synthesized perovskite catalysts was analyzed using an X-ray diffractometer (XRD) (D/MAX 2200V/PC, RIGAKU), and the structure of the perovskite oxides was

observed with a field-emission transmission electron microscope (FE-TEM) (JEM-2100F, JEOL). The electrochemical behaviors of the perovskite catalysts for the ORR and OER were investigated using a rotating disk electrode (RDE) and a potentiostat/galvanostat (PGSTAT302N, Autolab) in 0.5-M LiOH electrolyte. The perovskite oxides were mixed with deionized water and an ionomer (Nafion® 117 solution, Sigma-Aldrich), and the resulting mixture was loaded onto a glassy carbon RDE with an area of 0.071 cm². The counter and reference electrodes were a Pt plate and Hg/HgO/1-M NaOH, respectively. Linear sweep voltammetry (LSV) was conducted from 0.3 to -0.8 V for the ORR and from 0.3 to 0.8 V for the OER at a scan rate of 20 mV/s. The reactions' charge-transfer resistances were investigated via electrochemical impedance spectroscopy (EIS) (PGSTAT302N, FRA2 module). The rotation rate of the RDE for the ORR was fixed at 2,000 rpm.

3. RESULTS AND DISCUSSION

LaCoO₃ was prepared by three different methods: HT, CA, and AC. The crystal structures of the prepared catalysts were investigated using an XRD.

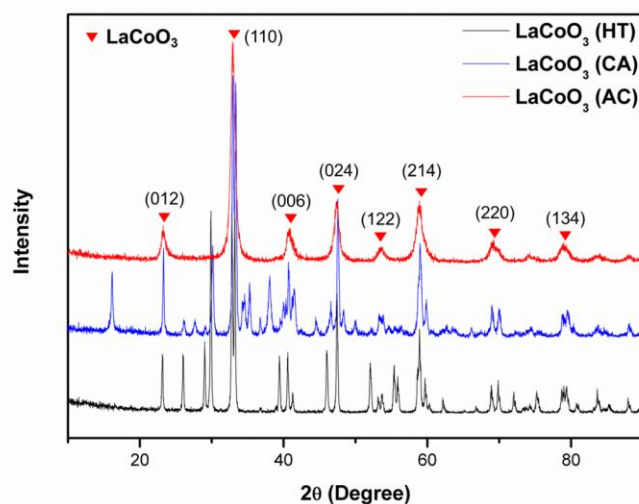


Figure 1. XRD patterns of LaCoO₃ catalysts prepared by three different methods: HT (black), CA (blue), and AC (red).

Figure 1 shows that LaCoO₃ perovskite was successfully prepared via HT and CA, but crystalline peaks from the precursor materials (La(NO₃)₃·6H₂O, Co(NO₃)₂·6H₂O, and La₂O₃) were present. Thus, these methods did not produce pure LaCoO₃ perovskite. However, AC resulted in pure LaCoO₃ perovskite, and the electrochemical characteristics this perovskite corresponded to those of pure perovskite.

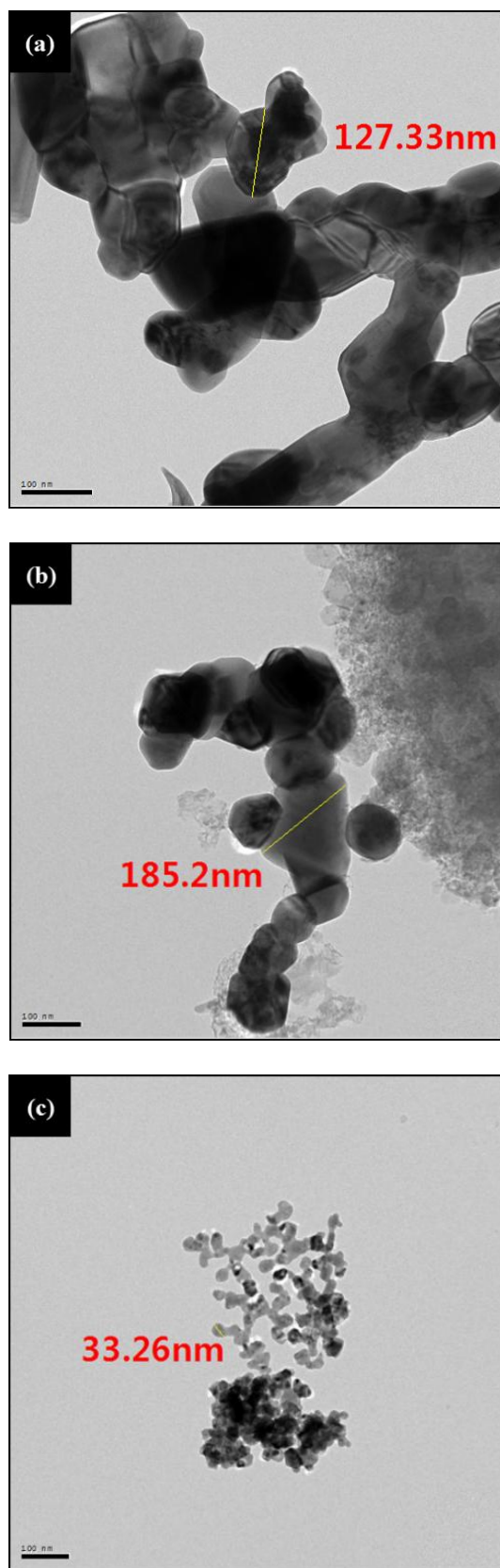


Figure 2. TEM images of LaCoO_3 catalysts prepared by three different methods: (a) HT, (b) CA, and (c) AC.

Figure 2 presents a TEM image showing that the average size of the LaCoO_3 (AC) was 33.26 nm; in contrast, the LaCoO_3 produced by HT and CA exhibited sizes exceeding 100 nm because of the agglomeration of different phases.

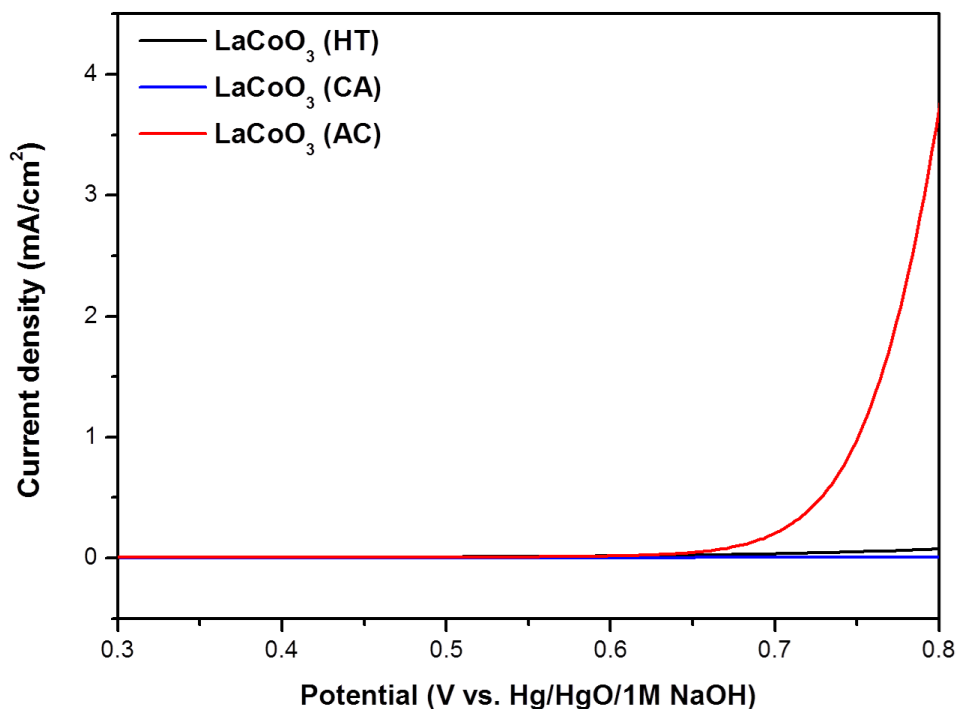


Figure 3. LSVs of LaCoO_3 catalysts for the OER: HT (black), CA (blue), and AC (red). Potential sweep rate: 20 mV/s.

The LSVs in Figure 3 show the effects of the perovskite preparation method on the resulting catalytic activity for the OER. Compared with LaCoO_3 prepared by HT and CA, LaCoO_3 prepared by AC showed excellent catalytic activity. The pure perovskite phase and small particle sizes achieved by AC are believed to be responsible for the high catalytic activity of the resulting material. Although the LaCoO_3 phase was produced by HT and CT, its coexistence with other crystalline phases may block its active sites. Thus, all subsequent experiments were performed with the LaCoO_3 catalyst obtained via AC.

To enhance the catalytic activities of the LaCoO_3 (AC) catalyst for the OER and ORR, the La of LaCoO_3 (AC) was partially substituted with Sr because Sr substitution at the A site of perovskite has been shown to increase the material's conductivity, O_2 diffusivity, and O_2 -dissociation ability, which could alter its electrocatalytic activities [14–15].

Figure 4 shows the XRD patterns of the $\text{La}_{1-x}\text{Sr}_x\text{CoO}_3$ catalysts. When the Sr substitution fraction, x , exceeds 0.5, peaks attributed to the $\text{Sr}(\text{NO}_3)_2$ and $\text{La}(\text{NO}_3)_2$ precursors start to appear, indicating that the limit of Sr insertion in the perovskite structure was reached. The catalytic activities of the $\text{La}_{1-x}\text{Sr}_x\text{CoO}_3$ catalysts were measured with LSV and are plotted in Figure 5.

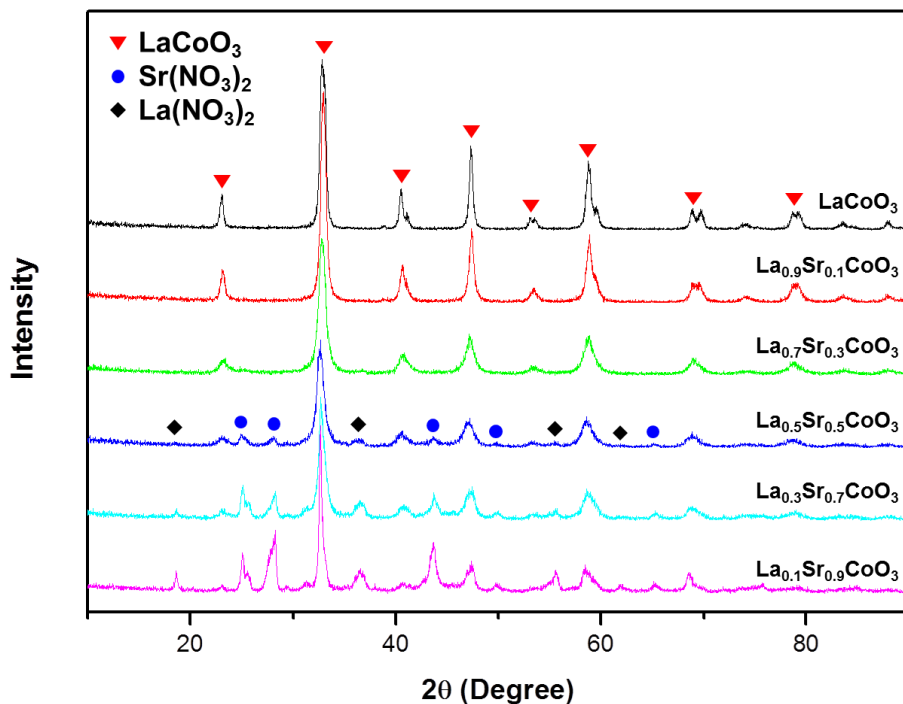


Figure 4. XRD patterns of La_{1-x}Sr_xCoO₃ with partial Sr substitution in the La-site of LaCoO₃ (AC).

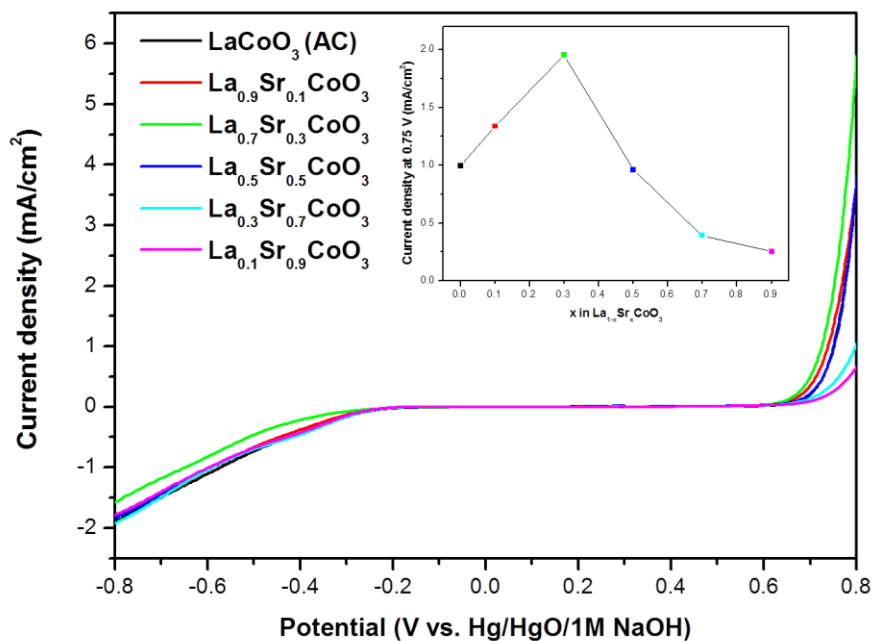


Figure 5. LSV of La_{1-x}Sr_xCoO₃ with partial Sr substitution in the La-site of LaCoO₃ (AC). Potential sweep rate: 20 mV/s.

The catalytic activity of $\text{La}_{1-x}\text{Sr}_x\text{CoO}_3$ for the OER varied with the extent of Sr^{+2} substitution, and the highest activity was obtained at $x=0.3$, *i.e.*, $\text{La}_{0.7}\text{Sr}_{0.3}\text{CoO}_3$. The inset of Figure 5 shows that, among the Sr^{+2} -substituted $\text{La}_{1-x}\text{Sr}_x\text{CoO}_3$ species, $\text{La}_{0.7}\text{Sr}_{0.3}\text{CoO}_3$ had the lowest onset potential and the highest anodic current value (0.75 V vs. Hg/HgO/1-M NaOH). Because the partial substitution of Sr^{+2} for La^{+3} requires the formation of oxide ion vacancies ($\text{La}_{1-x}^{+3}\text{Sr}_x^{+2}\text{Co}^{+3}\text{O}_{3-(x/2)}$), $\text{La}_{1-x}\text{Sr}_x\text{CoO}_3$ can be expected to exhibit higher catalytic activity as the Sr substitution increases because the generation of oxide ion vacancies increases the active lattice O [10,16]. However, it is unclear why the OER activities of $\text{La}_{1-x}\text{Sr}_x\text{CoO}_3$ were maximized at $x=0.3$.

In contrast, the catalytic activities of $\text{La}_{1-x}\text{Sr}_x\text{CoO}_3$ catalysts for ORR were low and were not significantly affected by Sr^{+2} substitution. $\text{La}_{0.7}\text{Sr}_{0.3}\text{CoO}_3$ that was highly active for the OER showed lower ORR catalytic activity, which can be ascribed to the decrease in the reactivity of the individual O species [10]. To increase the ORR activity while maintaining the high OER activity, 5 wt% Pt was loaded onto $\text{La}_{0.7}\text{Sr}_{0.3}\text{CoO}_3$ by a polyol method because Pt has the lowest overpotential for the ORR. Figure 6 shows that the Pt-loaded $\text{La}_{0.7}\text{Sr}_{0.3}\text{CoO}_3$ catalyst had higher ORR activity but slightly lower OER activity than $\text{La}_{0.7}\text{Sr}_{0.3}\text{CoO}_3$.

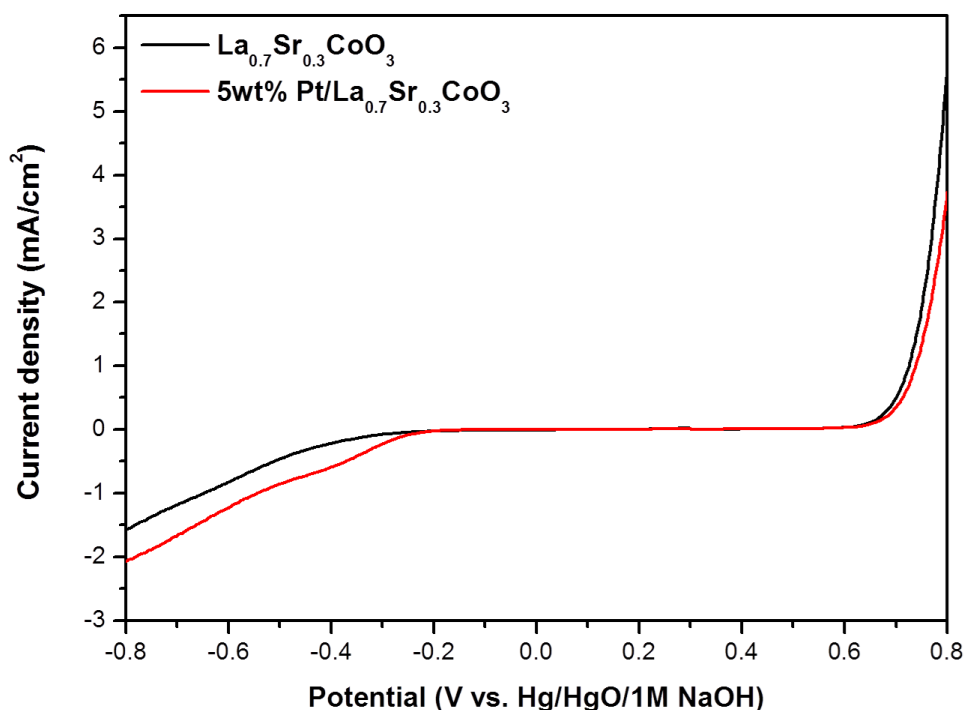


Figure 6. LSVs of $\text{La}_{0.7}\text{Sr}_{0.3}\text{CoO}_3$ and 5wt% Pt-loaded $\text{La}_{0.7}\text{Sr}_{0.3}\text{CoO}_3$ catalysts. Potential sweep rate: 20 mV/s.

Pt provides highly active sites for the ORR, but it can inhibit the OER by blocking the active sites of $\text{La}_{0.7}\text{Sr}_{0.3}\text{CoO}_3$. The charge-transfer resistances of the perovskite catalysts for the ORR and OER were measured by EIS over the frequency range of 100 kHz–0.01 Hz at -0.3 V and 0.75 V,

respectively. Figure 7 indicates that charge-transfer resistance of $\text{La}_{0.7}\text{Sr}_{0.3}\text{CoO}_3$ catalyst for the ORR can be significantly lowered by loading with Pt, but the charge-transfer resistance for the OER was similar for the Pt loaded and unloaded catalysts. It also shows that the charge-transfer resistance of the perovskite oxide for the OER was only 1/6 of that for the ORR. Figure 7 shows the EIS analysis results, which are in good agreement with the LSVs shown in Figure 6.

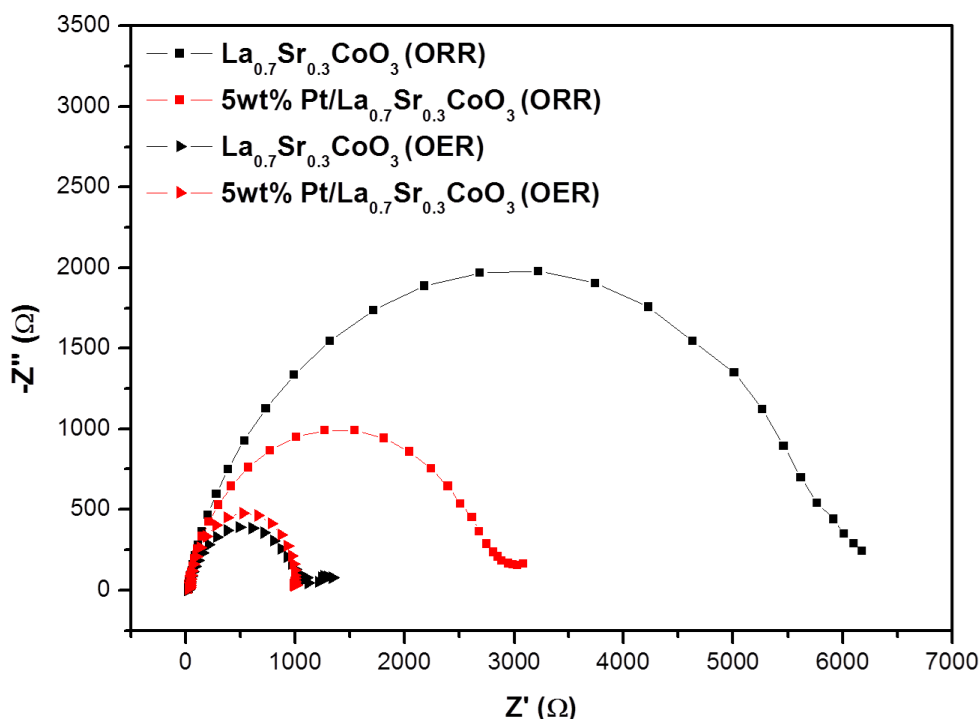


Figure 7. Nyquist plots of $\text{La}_{0.7}\text{Sr}_{0.3}\text{CoO}_3$ and 5wt% Pt-loaded $\text{La}_{0.7}\text{Sr}_{0.3}\text{CoO}_3$ catalysts for the ORR and OER.

4. CONCLUSIONS

The air electrodes of aqueous Li-air batteries should have high electrocatalytic activities for the ORR during discharging and the OER during charging. Perovskite oxide, ABO_3 , was investigated as a cathode material for aqueous Li-air batteries to replace noble metal catalysts, such as Pt and IrO_2 . Among the different synthesis methods used here, AC produced pure LaCoO_3 perovskite with small particle sizes at a relatively low calcination temperature (640°C). LaCoO_3 (AC) showed a high catalytic activity for the OER, and the La of LaCoO_3 was partially substituted with Sr to enhance the material's electrocatalytic activities for the ORR and OER. The LSV and EIS results of $\text{La}_{1-x}\text{Sr}_x\text{CoO}_3$ suggested that perovskite oxides are better electrocatalysts for the OER than for the ORR. $\text{La}_{0.7}\text{Sr}_{0.3}\text{CoO}_3$ showed excellent catalytic activity for the OER, and its ORR activity was enhanced by

loading it with 5 wt% Pt. Based on these results, perovskite materials are promising candidate materials for Li-air battery cathodes.

ACKNOWLEDGEMENTS

This research was supported by the New & Renewable Energy Core Technology Program of the Korea Institute of Energy Technology Evaluation and Planning (KETEP) with funding from the Ministry of Trade, Industry & Energy, Republic of Korea (Grant No. 20133030011320).

References

1. K. Abraham and Z. Jiang, *J. Electrochem. Soc.*, 143 (1996) 1.
2. P.C. Symons and P.C. Butler, *Introduction to Advanced Batteries for Emerging Applications*, Sandia National Lab Report SAND2001-2022P, Sandia National Laboratory, Albuquerque, NM, USA (available at http://infoserve.sandia.gov/sand_doc/2001/012022p.pdf). (2001).
3. G. Girishkumar, B. McCloskey, A. Luntz, and S. Swanson, and W. Wilcke, *J. Phys. Chem. Lett.*, 1 (2010) 2193.
4. S. Beattie, D. Manolescu, and S. Blair, *J. Electrochem. Soc.*, 156 (2009) A44.
5. A. Kraysberg and Y. Ein-Eli, *J. Power Sources*, 196 (2011) 886.
6. J. Lu, L. Li, J. Park, Y. Sun, F. Wu, and K. Amine, *Chem. Rev.*, 114 (2014) 5611.
7. D. Wittmaier, T. Danner, N. Wagner, and K.A. Friedrich, *J. Appl. Electrochem.*, 44 (2014) 73.
8. F. Cheng, J. Chen, *Chem. Soc. Rev.*, 41 (2012) 2172.
9. H. Choi, H. Jang, H. Hwang, M. Choi, D. Lim, S.E. Shim, and S-H. Baeck, *Electron. Mater. Lett.*, 10 (2014) 957.
10. H. Zhang, Y. Shimizu, Y. Teraoka, N. Miura, and N. Yamazoe, *J. Catal.*, 121 (1990) 432.
11. C.H. Kim, G. Qi, K. and Dahlberg, W. Li, *Science*, 327 (2010) 1624.
12. Z. Wang, D. Xu, J. Xu, and X. Zhang, *Chem. Soc. Rev.*, 43 (2014) 7746.
13. Y. Yamada, K. Yano, D. Hong, and S. Fukuzumi, *Phys. Chem. Chem. Phys.*, 14 (2012) 5753.
14. Y. Takeda, R. Kanno, M. Noda, Y. Tomida, and O. Yamamoto, *J. Electrochem. Soc.*, 134 (1987) 2656.
15. P. Ravindran, P. Korzhavyi, and H. Fjellvåg, A. Kjekshus, *Phys. Rev. B.*, 60 (1999) 16423.
16. Y. Tak, G. Lee, W. Lee, and H. Lee, *Korean Chem. Eng. Res.*, 26 (1988) 641.
17. E. Ghiasi, A. Malekzadeh, and M. Ghiasi, *J. Rare. Earth*, 31 (2013) 997.
18. M. Khazaei, A. Malekzadeh, F. Amini, Y. Mortazavi, and A. Khodadadi, *Cryst. Res. Technol.*, 45 (2010) 1064.
19. G. Kéranguéven, S. Royer, and E. Savinova, *Electrochem. Commun.* 50 (2015) 28.
20. Q. Wang, G.Q. Sun, L.H. Jiang, Q. Xin, S.G. Sun, Y.X. Jiang, S.P. Chen, Z. Jusys, and R.J. Behm, *Phys. Chem. Chem. Phys.* 9 (2007) 2686.

© 2016 The Authors. Published by ESG (www.electrochemsci.org). This article is an open access article distributed under the terms and conditions of the Creative Commons Attribution license (<http://creativecommons.org/licenses/by/4.0/>).